



OPEN ACCESS

EDITED BY

Kaiwen Sun,
University of New South Wales, Australia

REVIEWED BY

Yongli Lu,
Massachusetts Institute of Technology,
United States
Yinyan Liu,
University of New South Wales, Australia

*CORRESPONDENCE

Brahim Belmahdi,
✉ belmahdi.brahim@gmail.com

RECEIVED 24 September 2024

ACCEPTED 03 January 2025

PUBLISHED 20 January 2025

CITATION

Belmahdi B (2025) Comparative study of parameter extractions of photovoltaic modules using analytical and numerical approaches. *Front. Energy Res.* 13:1501335. doi: 10.3389/fenrg.2025.1501335

COPYRIGHT

© 2025 Belmahdi. This is an open-access article distributed under the terms of the [Creative Commons Attribution License \(CC BY\)](https://creativecommons.org/licenses/by/4.0/). The use, distribution or reproduction in other forums is permitted, provided the original author(s) and the copyright owner(s) are credited and that the original publication in this journal is cited, in accordance with accepted academic practice. No use, distribution or reproduction is permitted which does not comply with these terms.

Comparative study of parameter extractions of photovoltaic modules using analytical and numerical approaches

Brahim Belmahdi*

Abdelmalek Essaadi University, Tetouan, Morocco

Developing an accurate mathematical model for parameter extraction in photovoltaic modules is a crucial endeavor in optimizing photovoltaic energy systems. This study seeks to assess and compare various analytical and numerical methods for extracting the primary five parameters of photovoltaic modules. Specifically, six established approaches based on a single diode model (SDM) are employed, including the methods introduced by Khan et al., Blas et al., Phang et al., Vika, Cubas et al., and Almonacid et al. The performance of these approaches is evaluated and compared under standard test conditions (STC) with a focus on maximum power point current and voltage. The analytical and numerical methods demonstrate their precision in predicting photocurrent-voltage (I-V) and power-voltage (U-V) curves, with the exception of the Almonacid et al. method, which tends to underestimate the I-V curve at the module's maximum power. Among these methods, the Phang et al. approach stands out, displaying a strong agreement between experimental data and the predicted curve. This is evidenced by the lower values of root mean square error (RMSE), mean bias error (MBE), normalized RMSE (NRMSE), mean absolute percentage error (MAPE), and absolute error (AE). These findings underscore the high quality of results obtained through the Phang et al. method.

KEYWORDS

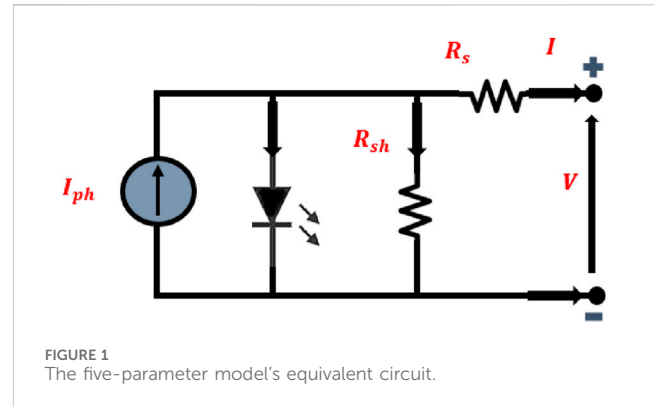
parameter extraction, photovoltaic modules, analytical/numerical approaches, single diode model, standard test conditions, I-V characteristics

1 Introduction

The escalating costs of fossil fuels and their detrimental impact on the environment, including air pollution resulting from greenhouse gas emissions like carbon dioxide and methane, have spurred global efforts to explore and develop clean and renewable energy technologies (Yahya-Khotbehsara and Shahhoseini, 2018). Solar energy, with its abundant intensity, offers a swift and straightforward means of conversion into photovoltaic (PV) electricity. This conversion leverages the inherent properties of semiconductors, making it a promising and effective renewable energy resource (Sheraz Khalid and Abido, 2014). In various energy conversion systems, it is possible to represent certain electrical photovoltaic (PV) characteristics using an equivalent electrical circuit. This approach is suitable for accurately emulating the actual behavior of solar cells, ensuring that the simulated data closely aligns with the measured current-voltage (I-V) data across all operational conditions (Chin et al., 2015). Among these representation methods, some well-known equivalent electrical circuits include the single diode model (SDM), double diode model (DDM), and

third diode model (TDM). These models have gained popularity and are employed by numerous researchers due to their high precision and performance. Moreover, the utilization of an increased number of parameters for extracting PV module characteristics within the single diode model enhances the accuracy of predicting the I-V behavior under varying solar radiation levels. This presents an intriguing opportunity in the research literature.

Parameter extraction methods can be categorized based on several factors, including the quantity of data samples involved in the extraction process, the specific method utilized, and the mathematical approach applied. In terms of the mathematical approach, the extraction of parameters from photovoltaic modules is typically classified into three main categories: numerical, analytical, and evolutionary methods. The primary objective of these methods is to establish a strong correlation and achieve an optimized fit between the theoretical and experimental I-V characteristics of solar cells (Yahya-Khotbehsara and Shahhoseini, 2018; Appelbaum and Peled, 2014). Given that a significant number of I-V data samples are utilized during the parameter extraction process, these optimization methods are considered to collectively result in substantial improvements in obtaining the final parameter values. The relevant literature offers a wealth of references on parameter extraction. An uncomplicated method for extracting the five parameters was introduced by Villalva et al. (2009), Cubas et al. is one of the most cited contributors in this field. Their technique, aimed at reducing the gap between estimated and experimental peak power values, involves incorporating the series resistance as a parameter. However, a limitation of this method is its use of a fixed ideality factor value of 1.3, which makes it more accurate in the vicinity of the maximum power point but less so in other regions (Cubas et al., 2014). Achouby et al. have introduced a comprehensive approach that utilizes four analytical formulas, along with certain approximations, to derive the values of four parameters. Additionally, it includes an ideality factor, which is typically defined to be around 1.3 (El Achouby et al., 2018). Zaimi et al. have developed a highly accurate numerical method for determining the five physical parameters of photovoltaic modules. This method involves fine-tuning the ideality parameter and enhancing a system of nonlinear equations. It's worth noting that the initial estimates for the four physical criteria in their method need to be precise for it to work effectively (Zaimi et al., 2019). Stornelli et al. have introduced an innovative approach that combines both numerical and well-established methodologies. In this method, it's essential to have consistent initial values for the shunt resistance and ideality factor, which are vital for its effectiveness. This approach presents a new and promising way to determine the five parameters of photovoltaic modules (Stornelli et al., 2019). This condensed technique allows for the identification of the ideal values for both the ideality parameter and the shunt resistance. Sera et al. (2008) Finding the ideal value of the ideality parameter and the shunt resistance is made possible by this condensed technique. The shunt resistance (R_{sh}) was advised to be disregarded by Sera et al. for the purpose of condensing the five-parameter model to a four-parameter model, Cannizzaro et al. (2014) proposed ignoring either R_s or R_{sh} . To make the computation simpler. Other analytical techniques call for more inputs, such as those in the Celik and Acikgoz (2007), Khan et al. (2013), and Bai et al. (2014) models, which call for extra



inputs of estimating or computing R_{sho} and R_{so} , or the slopes at both short-circuit (SC) and open-circuit (OC) locations. For the purpose of determining the five parameters, Batzelis and Papathanassiou (2016) and Saleem and Karmalkar (2009), Karmalkar and Haneefa (2008) also added new coefficients. Another approach was set forth by Bellia et al. (2014), Wang et al. (2017) and Hussein (2017) and is based on obtaining a closed-form equation for R_s and then numerically solving this expression for various ideality factor values. Iteratively calculating R_s , R_{sh} , and I_{ph} is the foundation of Vika's approach (Breisnes Vika, 2014).

In this study, the single diode model serves as a baseline for extracting parameters related to photo-generated current (I_{ph}), diode saturation current (I_0), diode ideality factor (α), series resistance (R_s), and shunt (or parallel) resistance (R_{sh}) under standard conditions (STC conditions, $G = 1000 \text{ W/m}^2$, $T = 25^\circ\text{C}$). Furthermore, the extracted parameters are employed to assess and compare six analytical/numerical methods, namely, the Khan et al. method, Blas et al. method, Phang et al. method, Vika method, Cubas et al. method, and Almonacid et al. method. The performance of these methods is analyzed using data sheets provided by the manufacturers of three main photovoltaic modules: the S70 and SM-210W polycrystalline, SP 75 and SPR-230 WHT-I monocrystalline, and Shell ST36 and U-EA110W thin film. All computations are conducted using Matlab software. The two sections of our study are as follows: The first section outlines the methods used by each author to extract the main five parameters of the single diode model, followed by an assessment and comparison of the effectiveness of each approach.

2 Theoretical base of analytical/numerical approaches

PV module performance accuracy is evaluated by examining the I-V characteristic under standard conditions. Various methods exist for modeling PV cells, offering different degrees of approximation to the actual device behavior. According to (Louzazni and Belmahdi, 2022), the SDM is the most commonly used approximation for PV module modeling. The SDM enables the extraction of five main parameters: the photo-generated current (I_{ph}), diode saturation current (I_0), diode ideality factor (α), series resistance (R_s), and shunt (or parallel) resistance (R_{sh}). These parameters are

TABLE 1 Electrical properties of three PV technologies.

PV modules	Polycrystalline (p-Si)		Monocrystalline (m-Si)		Thin film	
	S70	SM-210W	SP 75	SPR-230 WHT-I	Shell ST36	U-EA110W
Open-circuit voltage (V_{oc}) (V)	21.4	36.1	21.6	48.70	22.9	71
Short-circuit current (I_{sc}) (A)	4.7	7.93	4.7	5.99	2.86	2.50
Maximum power voltage (V_{MPP}) (V)	16.5	28.90	17.6	41.00	15.8	54.0
Maximum power current (I_{MPP}) (A)	4.25	7.28	4.26	5.61	2.28	2.04
Maximum power (P_{MPP}) (W)	70.125	210.4	75	230	44.6	116
Number of cells in series (N_s)	36	60	36	72	42	106
I_{sc} temperature coefficient ($\mu_{I_{sc}}$) (mA/°C)	2	4	2	3.5	0.320	1.375
V_{oc} temperature coefficient ($\mu_{V_{oc}}$) (mV/°C)	-76	-124	-76	-160.7	-100	-276.9

TABLE 2 Comparison of statistical metrics for evaluating PV module parameter extraction methods.

Metric	Definition	Purpose and key insights
RMSE	Measures the square root of the average of squared differences between experimental and predicted values	Quantifies the overall prediction error. Smaller values indicate better model performance. Sensitive to large errors, which are given more weight due to squaring
MAPE	Calculates the average of absolute percentage errors between experimental and predicted values	Evaluates the accuracy of predictions as a percentage. Useful for comparing across datasets with different scales Expresses error in relative terms but can be skewed by small experimental values
MBE	Computes the mean of the differences between experimental and predicted values	Indicates whether the model tends to overestimate or underestimate predictions Positive values suggest overestimation; negative values indicate underestimation
NRMSE	Normalizes the RMSE by dividing it by the range or mean of experimental data, often expressed as a percentage	Assesses prediction error relative to the magnitude of the data, allowing comparisons across datasets with different units or scales Provides scale-independent insight but depends on the normalization method used
AE	Represents the absolute difference between experimental and predicted values for individual data points	Focuses on localized deviations in the data, offering point-specific error analysis Useful for identifying outliers but does not provide an aggregate measure of model performance

TABLE 3 Effective normal irradiance, cell temperature, and the main electrical parameters derived from the I-V curves used for method evaluation.

G (W/m ²)	Tc (°C)	Curve	Polycrystalline (p-Si)				Monocrystalline (m-Si)				Thin film			
			S70		SM-210W		SP 75		SPR-230 WHT-I		Shell ST36		U-EA 110W	
			I_{sc} (A)	V_{oc} (V)	I_{sc} (A)	V_{oc} (V)	I_{sc} (A)	V_{oc} (V)	I_{sc} (A)	V_{oc} (V)	I_{sc} (A)	V_{oc} (V)	I_{sc} (A)	V_{oc} (V)
1,000	25	1	4.69	21.5	7.93	36.1	4.7	21.6	5.99	48.70	2.86	22.9	2.50	71

interrelated through a specific equation and are illustrated in Figure 1.

$$I = I_{ph} - I_0 \left(\exp \left(\frac{V + IR_s}{\alpha V_T} \right) - 1 \right) - \frac{V + IR_s}{IR_{sh}} \tag{1}$$

Where V_T is the thermal voltage of the PV cell, presented by the mathematical Equation 2:

$$V_T = \frac{kT}{q} \tag{2}$$

Where k and q is the Boltzmann constant ($k = 1.38E - 23$ J/K) and the elementary or electron charge ($q = 1.69E - 19$ C) respectively.

Concerning performance evaluation, the I-V characterization offers valuable insights into the crucial aspects of PV cells. In this context, the precise estimation of the parameters outlined in Equation 1 is detailed through the application of six methods namely, the Khan et al. method (Khan et al., 2013), Blas et al. method (De Blas et al., 2002), Phang et al. method (Phang et al., 1984), Vika method (Breisnes Vika, 2014), Cubas et al. method

TABLE 4 Parameters extraction of Polycrystalline (p-Si) module.

Methods		Parameters extraction	Polycrystalline (p-Si)	
			S70	SM-210W
Phang et al	Curve 1	I_0 (A)	$2.8587 \cdot 10^{-10}$	$3.62167 \cdot 10^{-10}$
		I_{ph} (A)	4.69054	7.9376
		R_s (Ω)	0.368	0.237
		R_{sh} (Ω)	134	141
		α	0.989	0.984
Blas et al	Curve 2	I_0 (A)	$4.8654 \cdot 10^{-10}$	$6.1067 \cdot 10^{-10}$
		I_{ph} (A)	4.70425	7.93657
		R_s (Ω)	0.348	0.373
		R_{sh} (Ω)	141	144
		α	1.005	1.005
Khan et al	Curve 3	I_0 (A)	$6.095687 \cdot 0.10^{-10}$	$7.68517 \cdot 0.10^{-10}$
		I_{ph} (A)	4.69931	7.93741
		R_s (Ω)	0.293	0.309
		R_{sh} (Ω)	145.617	139.240
		α	1.015	1.015
Vika	Curve 4	I_0 (A)	$7.54797 \cdot 10^{-10}$	$9.816493 \cdot 10^{-10}$
		I_{ph} (A)	4.71110	7.9315
		R_s (Ω)	0.396	0.187
		R_{sh} (Ω)	116	119
		α	1.027	1.026
Cubas et al	Curve 5	I_0 (A)	$9.377404 \cdot 10^{-10}$	$1.151188 \cdot 10^{-9}$
		I_{ph} (A)	4.7365542	7.93546
		R_s (Ω)	0.416	0.216
		R_{sh} (Ω)	144.98	147.01
		α	1.035	1.031
Almonacid et al	Curve 6	I_0 (A)	$1.45876 \cdot 0.10^{-07}$	$1.85651 \cdot 10^{-07}$
		I_{ph} (A)	4.72087	7.93768
		R_s (Ω)	0.471	0.487
		R_{sh} (Ω)	146.98	149.15
		α	1.335	1.330

(Cubas et al., 2014), and Femia et al. (Femia et al., 2012) method. The performance and effectiveness of these approaches are systematically assessed and compared under standard test conditions (STC conditions).

2.1 Khan et al. method

The Khan et al. method is an analytical technique specifically designed for parameter extraction from silicon solar cells. This

method focuses on obtaining parameters of PV cells under high radiation conditions. The extraction process involves utilizing initial values from key parameters such as I_{SC} , V_{oc} , I_{MPP} , V_{MPP} , R_{so} , and R_{sho} . The extraction is described by the following Equations 3–7:

$$I_o = \frac{\alpha V_T}{(R_{so} - R_s)} \exp\left(-\frac{V_{oc}}{\alpha V_T}\right) \tag{3}$$

$$R_s = R_{so} - \frac{V_{MPP} + R_{so} I_{MPP} - V_{oc}}{I_{MPP} + [\ln(I_{sc} - I_{MPP}) - \ln(I_{sc})] I_{sc}} \tag{4}$$

TABLE 5 Parameters extraction of Monocrystalline (m-Si) module.

Methods		Parameters extraction	Monocrystalline (m-Si)	
			SP 75	SPR-230 WHT-I
Phang et al	Curve 1	I_0 (A)	$2.5016 \cdot 10^{-11}$	$2.9320.25100.3214 \cdot 10^{-11}$
		I_{ph} (A)	4.70	5.99
		R_s (Ω)	0.350	0.251
		R_{sh} (Ω)	335	129
		α	0.981	1.001
Blas et al	Curve 2	I_0 (A)	$2.557 \cdot 10^{-11}$	$2.9431 \cdot 10^{-11}$
		I_{ph} (A)	4.70	5.99
		R_s (Ω)	0.370	0.321
		R_{sh} (Ω)	200	137
		α	0.999	0.999
Khan et al	Curve 3	I_0 (A)	$3.45687 \cdot 0.10^{-11}$	$3.71517 \cdot 0.10^{-11}$
		I_{ph} (A)	4.7541	5.99
		R_s (Ω)	0.390	0.390
		R_{sh} (Ω)	290	200
		α	1.005	1.005
Vika	Curve 4	I_0 (A)	$2.6256 \cdot 0.10^{-10}$	$2.94517 \cdot 0.10^{-10}$
		I_{ph} (A)	4.7096	5.9865
		R_s (Ω)	0.308	0.217
		R_{sh} (Ω)	298	120
		α	1.015	1.019
Cubas et al	Curve 5	I_0 (A)	$2.676229 \cdot 0.10^{-10}$	$2.966407 \cdot 0.10^{-10}$
		I_{ph} (A)	4.75181	5.98916
		R_s (Ω)	0.300	0.219
		R_{sh} (Ω)	200.35	119.43
		α	1.025	1.029
Almonacid et al	Curve 6	I_0 (A)	$5.58467 \cdot 10^{-09}$	1.698510^{-08}
		I_{ph} (A)	4.8765	5.8951
		R_s (Ω)	0.450	0.499
		R_{sh} (Ω)	221.32	200
		α	1.335	1.335

$$\alpha = \frac{V_{MPP} + R_s I_{MPP} - V_{oc}}{V_T [\ln(I_{sc} - I_{MPP}) - \ln(I_{sc})]} \tag{5}$$

$$R_{sho} = R_{sh} \tag{6}$$

$$I_{ph} = I_0 \exp\left(\frac{V_{oc}}{\alpha V_T} - 1\right) + \frac{V_{oc}}{R_{sh}} \tag{7}$$

2.2 Blas et al. method

The Blas et al. method is an analytical approach employed for the extraction of parameters associated with PV cell behavior. This method relies on a set of experimentally measured voltage-

TABLE 6 Parameters extraction of thin film module.

Methods		Parameters extraction	Thin film	
			Shell ST36	U-EA110W
Phang et al	Curve 1	I_0 (A)	1.264410 ⁻⁰⁹	1.25342 10 ⁻¹¹
		I_{ph} (A)	2.86	2.4576
		R_s (Ω)	0.348	0.398
		R_{sh} (Ω)	237	310
		α	0.983	0 0.999
Blas et al	Curve 2	I_0 (A)	1.9564. 10 ⁻⁰⁹	1.4845. 10 ⁻¹¹
		I_{ph} (A)	2.86	2.4976
		R_s (Ω)	0.415	0.572
		R_{sh} (Ω)	254	288
		α	1.005	1.005
Khan et al	Curve 3	I_0 (A)	2.45687 0.10 ⁻⁰⁹	2.08517 0.10 ⁻¹¹
		I_{ph} (A)	2.8612	2.5165
		R_s (Ω)	0.2615	0.469
		R_{sh} (Ω)	258.768	275.43
		α	1.015	1.020
Vika	Curve 4	I_0 (A)	2.905128. 10 ⁻⁰⁹	2.432145. 10 ⁻¹¹
		I_{ph} (A)	2.8598	2.497765
		R_s (Ω)	0.39876	0.266769
		R_{sh} (Ω)	217	235
		α	1.025	1.027
Cubas et al	Curve 5	I_0 (A)	3.422709 0.10 ⁻⁰⁹	2.930493 0.10 ⁻¹¹
		I_{ph} (A)	2.84986	2.5243
		R_s (Ω)	0.41866	0.4376
		R_{sh} (Ω)	246.88	246.99
		α	1.033	1.035
Almonacid et al	Curve 6	I_0 (A)	3.65467 10 ⁻⁰⁷	8.3654110 ⁻⁰⁹
		I_{ph} (A)	2.8652	2.5768
		R_s (Ω)	0.568	0.5791
		R_{sh} (Ω)	286.89	294.01
		α	1.335	1.335

intensity curves conducted under elevated temperature and high radiation levels. The values obtained from these experiments are then used to extract model parameters. Similar to the previously described method, the extraction of parameters from Equation 1 is performed for the specified temperature and solar radiation levels, utilizing initial values of I_{SC} , V_{oc} , I_{MPP} , V_{MPP} , R_{so} , and R_{sho} . The mathematical expression for this extraction process is provided as follows (Equations 8–11):

$$I_o = \left(\left(I_{sc} \left(1 + \frac{R_s}{R_{sh}} \right) - \frac{V_{oc}}{R_{sh}} \right) \exp \left(- \frac{V_{oc}}{\alpha V_T} \right) \right) \tag{8}$$

$$R_s = \frac{R_{so} \left(\frac{V_{oc}}{\alpha V_T} - 1 \right) + R_{so} \left(1 - \frac{I_{sc} R_{so}}{\alpha V_T} \right)}{\frac{V_{oc} - I_{sc} R_{so}}{\alpha V_T}} \tag{9}$$

$$\alpha = \frac{V_{MPP} + R_s I_{MPP} - V_{oc}}{V_T \ln \left[\frac{(I_{sc} - I_{MPP}) \left(1 + \frac{R_s}{R_{sh}} \right) \frac{V_{MPP}}{R_{sh}}}{I_{sc} \left(1 + \frac{R_s}{R_{sh}} \right) \frac{V_{oc}}{R_{sh}}} \right]} \tag{10}$$

$$R_{sh} = R_{sho} - R_s \tag{11}$$

The calculation of I_{ph} is determined as per the definition in Equation 7. The computational procedure for this method involves several steps:

1. Initial value assignment for R_s .
2. Approximate estimation of both R_{sho} and α values.
3. Recalculation of R_s based on the obtained estimates.
4. Iterative repetition of step 3 until R_s converges to a stable value.

The remaining measured data has been discussed in previous sections.

2.3 Phang et al. method

The Phang et al. method is an analytical approach designed for the extraction of the primary five parameters from different single-junction PV cells under standard levels of solar radiation and cell temperature. The estimation of R_{sho} and R_{so} involves implementing a linear fit of the I-V curve around both the short-circuit current and open-circuit voltage, enabling the following (Equations 12, 13):

$$R_{sho} = -\left(\frac{dV}{dI}\right)_{I=I_{sc}} \tag{12}$$

$$R_{so} = -\left(\frac{dV}{dI}\right)_{V=V_{oc}} \tag{13}$$

The parameters of Equation 1 are estimated and given as follows (Equations 14–16):

$$I_0 = \left(I_{sc} - \frac{V_{oc}}{R_{sh}}\right) \exp\left(\frac{V_{oc}}{\alpha V_T}\right)$$

$$I_{ph} = I_{sc} \left(1 + \frac{R_s}{R_{sh}}\right) + I_0 \left(\exp\left(\frac{I_{sc} R_s}{\alpha V_T}\right) - 1\right) \tag{14}$$

$$R_s = R_{so} - \frac{\alpha V_T}{I_0} \exp\left(-\frac{V_{oc}}{\alpha V_T}\right) \tag{15}$$

$$\alpha = \frac{V_{MPP} + R_{so} I_{MPP} - V_{oc}}{V_T \left[\ln\left(I_{sc} - I_{MPP} - \frac{V_{MPP}}{R_{sh}}\right) - \ln\left(I_{sc} - \frac{V_{oc}}{I_{sc} - \frac{I_{MPP}}{R_{sh}}}\right) \right]} \tag{16}$$

The value of R_{sh} is estimated as previously defined in Equation 6.

2.4 Vika method

The Vika method, also known as the Vika algorithm, is employed for the extraction of parameters from PV cells under standard solar radiation and cell temperature conditions. This method involves fitting the dataset adequately for a specified number of iterations, incorporating variables such as R_s, I_{ph}, R_{sh} . The initial values of $I_{SC}, V_{oc}, I_{MPP}, V_{MPP}, R_{so},$ and R_{sho} are computed according to the following mathematical expression Equations 17–20:

$$I_0 = \frac{I_{sc}}{\exp\left(\frac{V_{oc}}{\alpha V_T}\right) - 1} \tag{17}$$

$$I_{ph} = I_{sc} \left(\frac{R_{sh} + R_s}{R_{sh}}\right) \tag{18}$$

$$R_s = \frac{V_{MPP}}{I_{MPP}} - \frac{\alpha V_T R_{sh}}{I_0 R_{sh} \left[\exp\left(\frac{V_{MPP} + I_{MPP} R_s}{\alpha V_T}\right) - 1\right]} \tag{19}$$

$$R_{sh} = \frac{V_{MPP} + I_{MPP} R_s}{I_{ph} - I_{MPP} - I_0 \left[\exp\left(\frac{V_{MPP} + I_{MPP} R_s}{\alpha V_T}\right) - 1\right]} \tag{20}$$

2.5 Cubas et al. method

The Cubas et al. method is an analytical technique designed to extract parameters for various types of PV technology under standard levels of radiation and cell temperature. Similar to the previously discussed methods, the extraction of parameters from Equation 1 is estimated using initial values of $I_{SC}, V_{oc}, I_{MPP}, V_{MPP}, R_{so},$ and R_{sho} . This estimation is accomplished through the following Equations 21–23:

$$I_0 = \frac{I_{sc} (R_{sh} + R_s) - V_{oc}}{R_{sh} \exp\left(\frac{V_{oc}}{\alpha V_T}\right)} \tag{21}$$

$$I_{ph} = I_{sc} \left(\frac{R_{sh} + R_s}{R_{sh}}\right) \tag{22}$$

$$R_{sh} = \frac{(V_{MPP} - I_{MPP} R_s)(V_{MPP} - R_s(I_{sc} - I_{MPP}) - \alpha V_T)}{(V_{MPP} - I_{MPP} R_s)(I_{sc} - I_{MPP}) - \alpha V_T} \tag{23}$$

2.6 Almonacid et al. Method

The Almonacid et al. (2016) method is a numerical approach employed for the extraction of parameters from PV cells. This method is based on a developed system with non-linear implicit equations derived from Equation 1. Within this system, the primary five unknown parameters are solved using the trust-region optimization algorithm (Powell, 1968). This algorithm enhances robustness, especially when dealing with initial values that are far from the solution. Additionally, it can handle cases where the Jacobian becomes singular at a specific iteration. The initial values of $I_{SC}, V_{oc}, I_{MPP}, V_{MPP}, R_{so},$ and R_{sho} are calculated using the following mathematical expression Equations 24–27:

$$I_0 = \left(I_{sc} - \frac{V_{oc} - R_s I_{sc}}{R_{sh}}\right) \exp\left(\frac{V_{oc}}{\alpha V_T}\right) \tag{24}$$

$$I_{ph} = I_{sc} \left(1 + \frac{R_s}{R_{sh}}\right) \tag{25}$$

$$R_s = R_{so} - \frac{\alpha V_T}{I_{sc} - \frac{V_{oc}}{R_{sh}}} \tag{26}$$

$$R_{sh} = R_{sho} \tag{27}$$

In the Vika, Cubas et al., and Almonacid et al. methods, the parameter α remains unidentified. To address this, multiple trials are conducted to solve the equation system within a defined interval [0.1, 1.5], with the α parameter changing in increments of 0.1. The solutions obtained through these trials are then regarded as the extracted parameters of the I-V curve.

TABLE 7 Statistical metric of all proposed methods for three different technologies.

A	Polycrystalline (P-Si)							
	S-70				SM-210W			
	RMSE	MBE	MAPE	NRMSE	RMSE	MBE	MAPE	NRMSE
Phang et al	0.05897	-1.37639	0.03150	0.11794	0.04209	-1.44328	0.03071	0.08418
Blas et al	0.06378	-1.33871	0.04644	0.12756	0.04186	-1.34239	0.04524	0.08372
Khan et al	0.07078	-1.06739	0.05660	0.14156	0.05967	-1.15508	0.05564	0.11934
Vika	0.07946	-0.91824	0.07406	0.15892	0.06806	-0.93922	0.07157	0.13612
Cubas et al	0.08093	-0.57138	0.09201	0.16186	0.14563	-0.57800	0.09101	0.29126
Almonacid et al	0.12953	-0.43996	0.13264	0.25906	0.24452	-0.45431	0.13196	0.48904
B	Monocrystalline (M-Si)							
	SP-75				SPR-230 WHT-I			
	RMSE	MBE	MAPE	NRMSE	RMSE	MBE	MAPE	NRMSE
Phang et al	0.03874	-1,54,819	0.02752	0.07748	0.02378	-1,55,512	0.02050	0.04756
Blas et al	0.03772	-1,34,497	0.04502	0.07544	0.02148	-1,3596	0.04450	0.04296
Khan et al	0.03592	-1,16,796	0.05384	0.07184	0.02017	-1,1951	0.04958	0.04034
Vika	0.03144	-0,96,205	0.07117	0.06288	0.01958	-0,97,487	0.07049	0.03916
Cubas et al	0.13093	-0,58,957	0.08897	0.26186	0.19033	-0,65,874	0.08502	0.38066
Almonacid et al	0.23043	-0,46,891	0.12966	0.46086	0.20169	-0,48,499	0.11671	0.40338
C	Thin film							
	ST36				U-EA110W			
	RMSE	MBE	MAPE	NRMSE	RMSE	MBE	MAPE	NRMSE
Phang et al	0.07432	-1.36033	0.03990	0.14864	0.06558	-1.36903	0.03814	0.13116
Blas et al	0.07975	-1.23238	0.04955	0.1595	0.06986	-1.24420	0.04903	0.13972
Khan et al	0.08107	-0.99686	0.06973	0.16214	0.07571	-1.00057	0.06781	0.15142
Vika	0.07979	-0.84197	0.08017	0.15958	0.07885	-0.89227	0.07777	0.1577
Cubas et al	0.09337	-0.52920	0.10790	0.18674	0.12930	-0.54946	0.10551	0.2586
Almonacid et al	0.16369	-0.40241	0.13899	0.32738	0.28078	-0.41910	0.13691	0.56156

The selected methods were chosen for their established accuracy, reliability, and relevance to the study's objectives. Each method offers unique strengths that make it suitable for analyzing PV systems. Phang et al. is renowned for accurately modeling I-V and P-V curves near the maximum power point, ensuring reliable performance evaluation across different PV technologies. Blas et al. provides detailed modeling that incorporates environmental factors, making it applicable in diverse climatic conditions. Khan et al. focuses on computationally efficient approaches, ideal for real-time or large-scale applications. Vika contributes valuable insights into system behaviors and environmental interactions, while Cubas et al. emphasizes parameter extraction and practical implementation for accurate and dependable results. Together,

these methods offer a comprehensive and balanced evaluation framework.

3 Result and discussion

To examine the outcomes obtained from the analytical/numerical methods discussed in the preceding section, MATLAB software was employed to estimate the primary five parameters extracted using the SDM for three distinct PV module technologies. These technologies include polycrystalline (p-Si), monocrystalline (m-Si), and thin film. The performance of the selected methods is evaluated based on the electrical characteristics at STCs, manufacturing conditions, and the temperature coefficients for

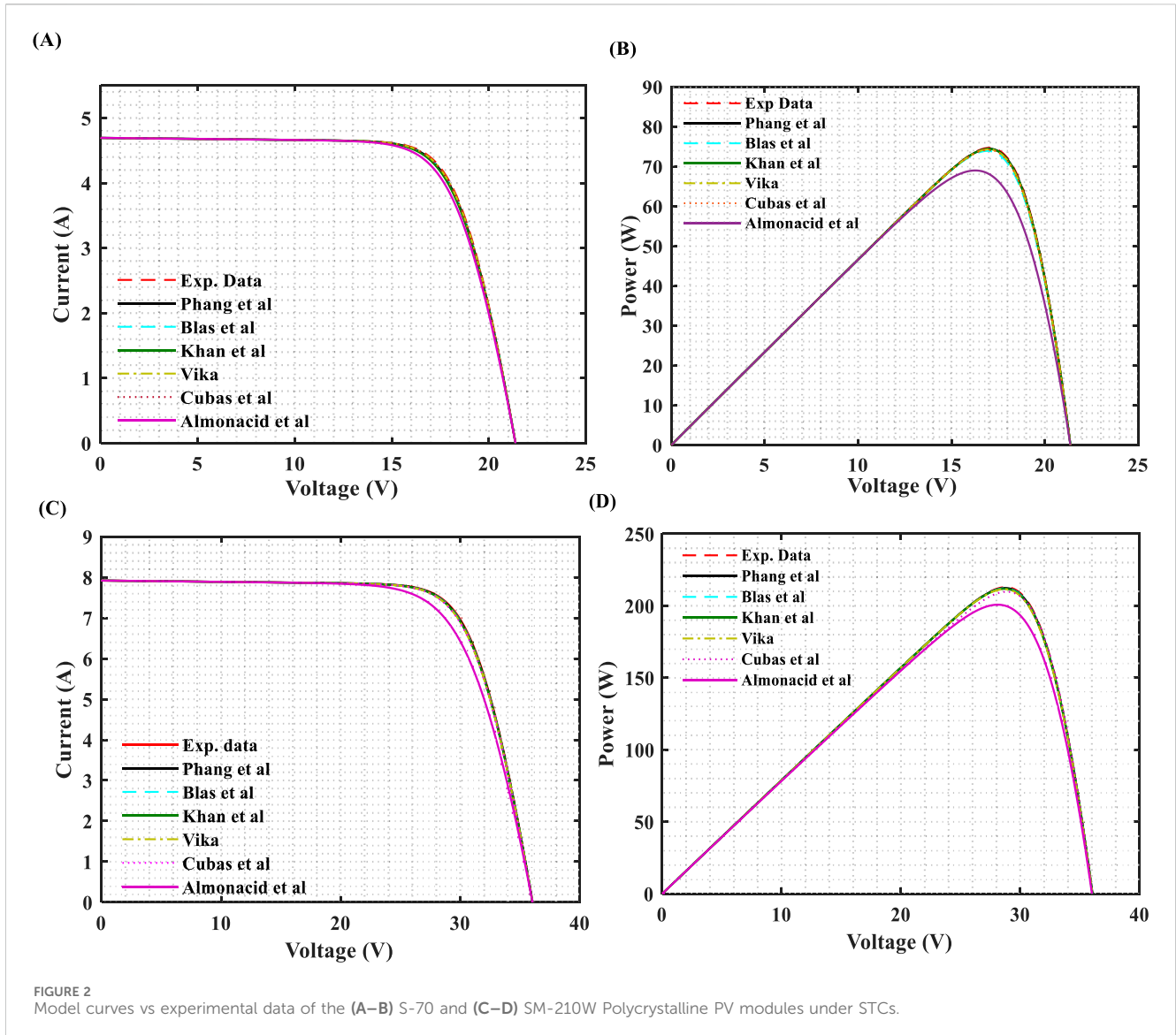


FIGURE 2 Model curves vs experimental data of the (A–B) S-70 and (C–D) SM-210W Polycrystalline PV modules under STCs.

the maximum power point (MPP) of the utilized photovoltaic modules, as outlined in Table 1.

To evaluate and compare the selected methods, various statistical metrics are employed to gauge the precision of our analytical/numerical approaches for extracting parameters from PV modules operating under STCs and manufacturing conditions. The primary statistical metrics include root mean square error (RMSE), mean bias error (MBE), mean absolute percentage error (MAPE), normalized root mean square error (NRMSE), and Absolute error (AE). The mathematical expressions (Equations 28–32) for these statistical metrics are provided as follows:

$$RMSE = \sqrt{\frac{1}{N} \sum_{i=1}^N (I_{Experimental} - I_{Computed})^2} \quad (28)$$

$$MBE = \frac{1}{N} \sum_{i=1}^N \left| \frac{(I_{Experimental} - I_{Computed})}{I_{Experimental}} \right| \quad (29)$$

$$MAPE = \frac{1}{N} \sum_{i=1}^N | (I_{Experimental} - I_{Computed}) | \quad (30)$$

$$NRMSE = \frac{\sqrt{\frac{1}{N} \sum_{i=1}^N (I_{Experimental} - I_{Computed})^2}}{\frac{1}{N} \sum_{i=1}^N (I_{Experimental})} \quad (31)$$

$$AE = | I_{Experimental} - I_{Computed} | \quad (32)$$

Where $I_{Experimental}$, and $I_{Computed}$ are the experimental and computed current, respectively. N is the number of experimental/computed currents. Table 2 below explaining the main differences between the selected statistical metrics (RMSE, MBE, MAPE, NRMSE, and AE) in the context of photovoltaic (PV) module analysis. It is noted that a lower value of these statistical indicator metrics indicates that the selected methods are suitable for extracting parameters from PV modules.

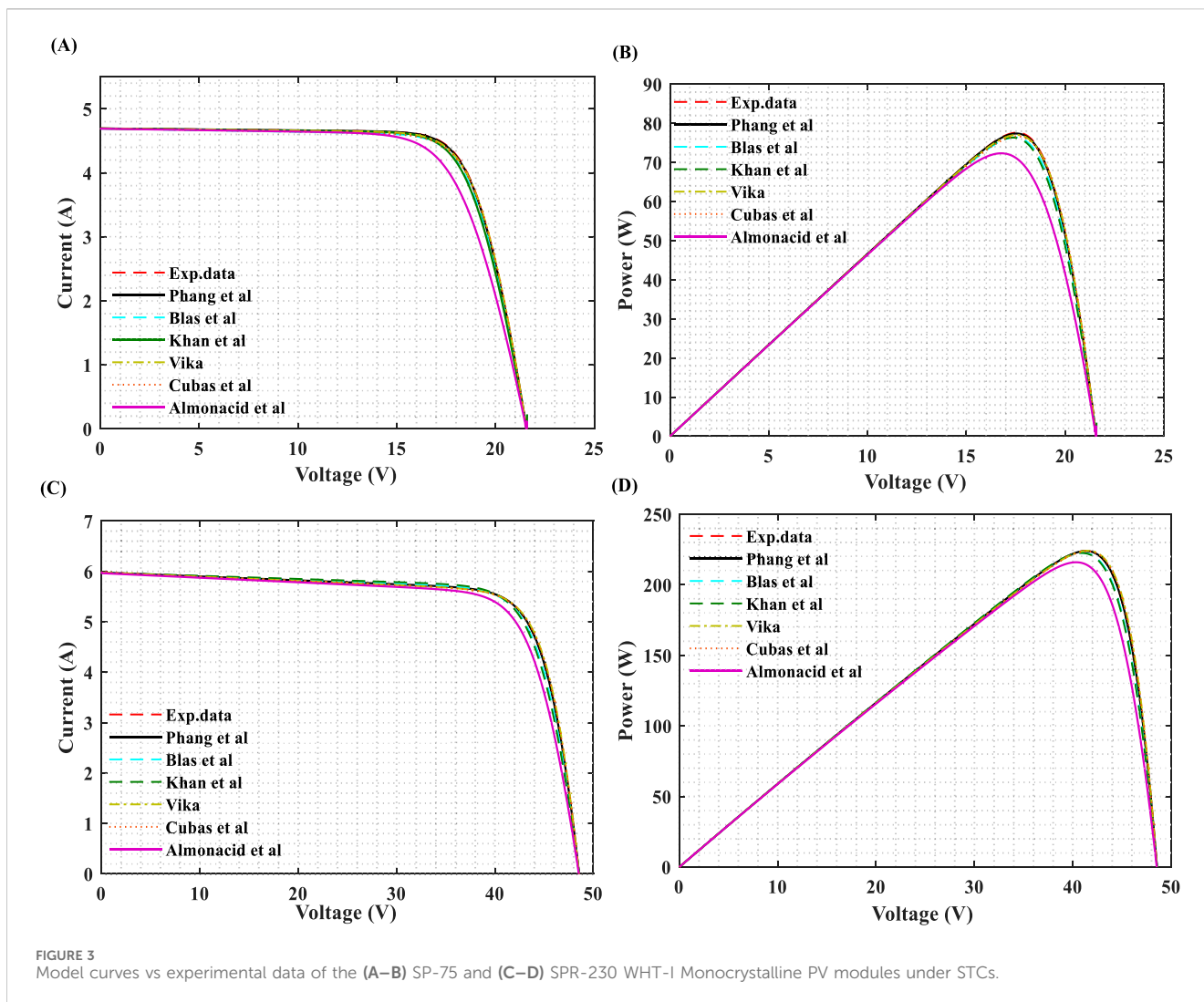


FIGURE 3 Model curves vs experimental data of the (A–B) SP-75 and (C–D) SPR-230 WHT-I Monocrystalline PV modules under STCs.

In this section, the analysis of the results obtained from the methods described in the previous section is presented. To facilitate this analysis, several I-V curves spanning the full operational range of the PV technologies were selected. Initially, the recorded I-V curves were analyzed as a function of cell temperature and effective irradiance.

Based on this analysis, the I-V curves presented in Table 3 were identified as a representative dataset for the various photovoltaic (PV) technologies under real operating conditions. Specifically, Curve 1 corresponds to I-V curves near the peak of the data distribution, representing typical working conditions for the PV modules. Further details on these representative I-V curves can be found in Table 3. The criteria above, as well as the I-V curves shown in Table 3, are the same previously considered by the authors to validate the models analyzed in (Almonacid et al., 2016).

The main findings of the analytical/numerical methods are presented in Tables 4–6, respectively. It is evident from Tables 4–6 that the predictions of all selected methods are approximately the same for the assessment of I_{ph} . Regarding I_0 , Phang et al., Vika, Cubas et al., Khan et al., and Blas et al. methods tend to predict the highest and lowest values. The range values of the considered methods are between 1.264410^{-09} A and $4.266407 \cdot 10^{-11}$ A

respectively, and are appropriate for p-Si, m-Si, and thin film technologies. Phang et al. indicates that the prediction results are approximately closer, while the previous methods still lead to showing the highest values (The range value is between 8.3654110^{-09} A and $3.65467 \cdot 10^{-07}$ A).

In terms of the ideality factor, the estimated value of α is technology-dependent (p-Si, m-Pi, and thin film). It is clear from the three technologies of PV modules that all proposed methods predict a significant value of the ideality factor except for the last (Almonacid et al.) method. The range values of Phang et al., Vika, Cubas et al., Khan et al., and Blas et al. methods are between 0.983 and 1.335 for the three technologies. The Almonacid et al. method presents almost the same prediction values with a slight variation, which is higher compared to the other methods.

According to Tables 4–6, Phang et al., Vika, Cubas et al., Khan et al., and Blas et al. methods surpass the Almonacid et al. methods in terms of R_s and R_{sh} . The range value of R_s and R_{sh} for appropriate methods are respectively between 0.187 Ω and 0.510 Ω , 116 Ω and 275 Ω for the three technology.

To evaluate the performance accuracy of each method under standard conditions ($GNI = 1000 \text{ W/m}^2$, $T = 25^\circ\text{C}$), the figures below

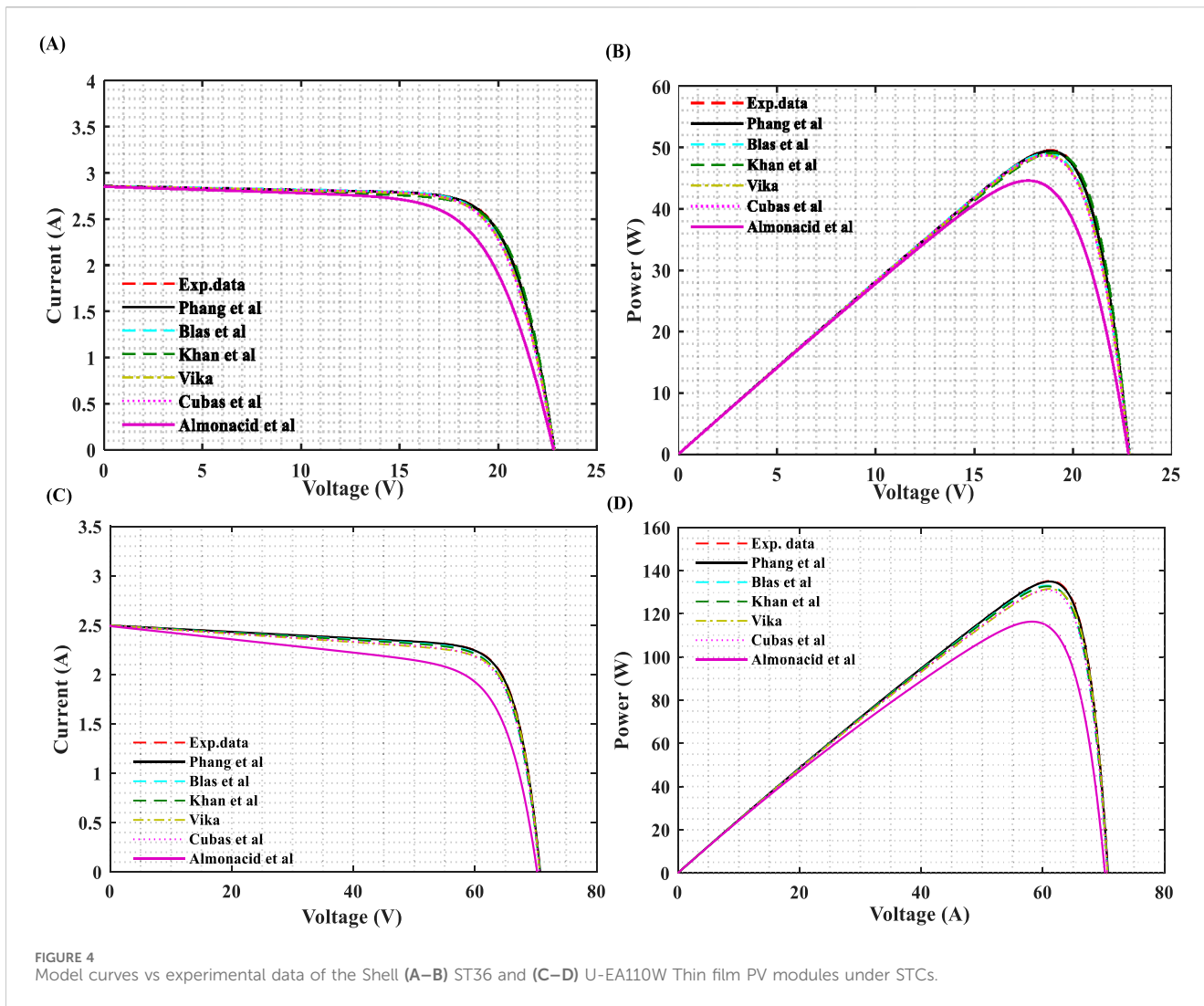


FIGURE 4 Model curves vs experimental data of the Shell (A–B) ST36 and (C–D) U-EA110W Thin film PV modules under STCs.

depict both I-V and P-V curves for three technologies (polycrystalline, monocrystalline, and thin film). As evident from the figures, all the proposed methods exhibit well-fitted curves, indicating good agreement with experimental data at standard conditions. Notably, the Almonacid et al. method for the three technologies demonstrates the least favorable curve compared to the preceding methods.

Figures 2A–D depicts the I-V and P-V curves of S-70 and SM-210W p-Si PV modules generated by six methods under STC conditions. The predictive methods exhibit high performance across all methods, excluding the Almonacid et al. method. Considering both Table 7 and Figures 2A–D, Phang et al., Blas et al., Khan et al., and Vika methods are deemed appropriate, closely aligning with experimental data. The range values of RMSE (%), MBE (%), and MAPE are 0.080575, -0.95201166, and 0.0722083 for S-70, and 0.20266, 0.98897, and 0.10125 for SM-210W polycrystalline PV modules, respectively. In terms of I-V and P-V curves, the Cubas et al. method exhibits a slight variation compared to the preceding methods. The Almonacid et al. method records the highest value of NRMSE, approximately 0.25906 and 0.48904 for S-70 and SM-210W, respectively. The results obtained from the single diode model for polycrystalline modules indicate

that the SM-210W module is more accurate compared to the S-70 PV module.

Figures 3A–D provides a comparative analysis of six proposed methods for SP-75 (A-B) and SPR-230 WHT-I (C-D) monocrystalline PV modules under STCs. This figure illustrates the I-V and P-V curves for each method, highlighting the relationship between the prediction methods and experimental data. Referring to Table 7 and Figures 3A–D, the maximum and minimum values of RMSE (%) vary between 0.23043 and 0.03144 for SP-75 monocrystalline silicon and 0.20169 and 0.01958 for SPR-230 WHT-I monocrystalline silicon, respectively. The range values of RMSE (%) suggest that the Phang et al., Blas et al., Khan et al., Vika, and Cubas et al. methods exhibit smaller values than the Almonacid et al. method. In terms of I-V and P-V curves for SP-75 and SPR-230 WHT-I monocrystalline PV modules, the methods depicted in Figures 3A–D closely align with the experimental data, earning recognition as “the most accurate prediction methods” compared to the S-70 and SM-210W polycrystalline PV modules.

Figures 4A–D and Table 7 present the prediction accuracy of Phang et al., Blas et al., Khan et al., Vika, Cubas et al., and Almonacid et al. methods under STCs for (A-B) ST36 and (C-D) U-EA110W

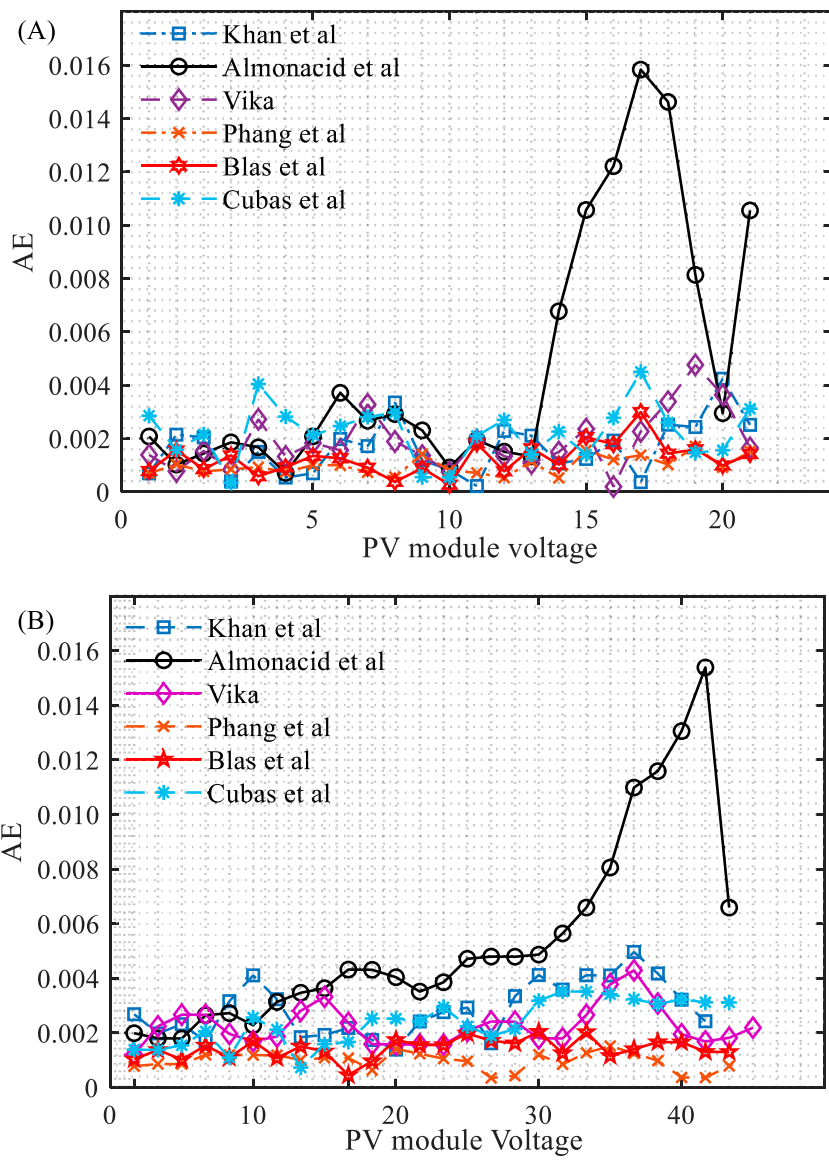


FIGURE 5 Absolute Error vs PV module voltage of SDM for (A) SP-75 and (B) SPR-230 WHT-I monocrystalline at STCs.

thin film PV modules. Among the six methods, Phang et al., Blas et al., Khan et al., Vika, and Cubas et al. exhibit the lowest values of MBE (%), MBE (%), MAPE, and RMSE. In terms of I-V and P-V curves, all five methods curve well compared to the Almonacid et al. method and closely align with the experimental data. It is evident from the table that the U-EA110W thin film PV module is more accurate compared to the ST36 thin film PV module. Similarly, consistent with the previous prediction methods, thin film PV modules are recognized as “the least accurate prediction methods” compared to monocrystalline and polycrystalline PV modules.

Table 7 provides numerical values for the selected methods, employing computational performance analysis to compare and evaluate their accuracy in predicting experimental data for monocrystalline, polycrystalline, and thin film PV modules. The results show that all methods, except for Almonacid et al., exhibit

lower prediction errors for the three PV technologies at the maximum power point. It is important to note that there is no specific criterion for determining which method is more appropriate, as no technique consistently outperforms the others under all conditions. Nevertheless, the Phang et al. method demonstrated a strong alignment with experimental I-V and P-V curves, particularly near the maximum power point, based on lower RMSE, MAPE, and AE values across all PV technologies. Thus, it can be regarded as a suitable approach for all three technologies. It is worth mentioning that our findings align with those studied in (Phang et al., 1984; Chan et al., 1986), where analytical methods are highlighted for their strong performance, closely matching fitting curves and numerical methods under standard STC conditions.

In this section, the optimal technology for a SDM is illustrated in Figures 5A,B. The figures depict the AE versus PV module voltage for both SP-75 and SPR-230 WHT-I monocrystalline PV modules

using various methods. The maximum AE values are 0.004238 for Phang et al., 0.015832 for Almonacid et al., 0.005772 for Vika, 0.001702 for Khan et al., 0.003988 for Blas et al., and 0.004598 for Cubas et al. in the case of SP-75. Similarly, for SPR-230 WHT-I, the maximum AE values are 0.004958 for Phang et al., 0.015381 for Almonacid et al., 0.004286 for Vika, 0.000151 for Khan et al., 0.00204 for Blas et al., and 0.003514 for Cubas et al. method.

The parameter extraction for the SDM of three different photovoltaic modules has been presented, with the first five analytical/numerical methods identified as suitable models based on their lower values of several statistical metrics, particularly the Phang et al. and Blas et al. methods. The Phang et al. method, in particular, achieves high accuracy through its use of a linear fit near critical points, such as the short-circuit current and open-circuit voltage. This approach enhances its robustness in minimizing errors across different PV technologies and demonstrates strong agreement between experimental data and the predicted curves. These attributes underscore the high quality and reliability of the results obtained using the Phang et al. method for the proposed technologies.

4 Conclusion

This paper provides a comparative study of various analytical/numerical methods for estimating parameter extraction in different technologies of PV modules. The simulations were conducted under STCs using a single diode model implemented in the Matlab Environment software. Each method was introduced and modeled, and their appropriateness was assessed based on statistical metrics such as RMSE, NRMSE, MAPE, MBE, and AE.

The performance analysis of the six methods was tested across different manufacturers of monocrystalline, polycrystalline, and thin film modules. The I-V and P-V curves of all selected methods exhibited a strong relationship between experimental and predicted values, except for the Almonacid et al. method. Notably, the Phang et al., Blas et al., Khan et al., and Vika methods demonstrated lower error values for various PV modules, including S-70 and SM-210W polycrystalline, SP 75 SPR-230 WHT-I Monocrystalline, and Shell ST36 and U-EA110W thin film modules. Conversely, the Almonacid et al. method yielded the highest error values compared to the other methods.

References

- Almonacid, F., Rodrigo, P., and Energy, E. F. (2016). *undefined: determination of the current-voltage characteristics of concentrator systems by using different adapted conventional techniques*. Elsevier.
- Appelbaum, J., and Peled, A. (2014). Parameters extraction of solar cells - a comparative examination of three methods. *Sol. Energy Mater. Sol. Cells*. 122, 164–173. doi:10.1016/j.solmat.2013.11.011
- Bai, J., Liu, S., Hao, Y., Zhang, Z., Jiang, M., and Zhang, Y. (2014). Development of a new compound method to extract the five parameters of PV modules. *Energy Convers. Manag.* 79, 294–303. doi:10.1016/j.enconman.2013.12.041
- Batzelis, E. I., and Papanthassiou, S. A. (2016). A method for the analytical extraction of the single-diode PV model parameters. *IEEE Trans. Sustain. Energy*. 7, 504–512. doi:10.1109/TSTE.2015.2503435
- Bellia, H., Youcef, R., and Fatima, M. (2014). A detailed modeling of photovoltaic module using MATLAB. *NRIAG J. Astron. Geophys.* 3, 53–61. doi:10.1016/j.nriag.2014.04.001
- Breisnes Vika, H. (2014). *Modelling of photovoltaic modules with battery energy storage in simulink/matlab with in-situ measurement comparisons*.
- Cannizzaro, S., Di Piazza, M. C., Luna, M., and Vitale, G. (2014). "Generalized classification of PV modules by simplified single-diode models," in *IEEE international symposium on industrial electronics* (Institute of Electrical and Electronics Engineers Inc.), 2266–2273. doi:10.1109/ISIE.2014.6864971
- Celik, A. N., and Acikgoz, N. (2007). Modelling and experimental verification of the operating current of mono-crystalline photovoltaic modules using four- and five-parameter models. *Appl. Energy*. 84, 1–15. doi:10.1016/j.apenergy.2006.04.007
- Chan, D. S. H., Phillips, J. R., and Phang, J. C. H. (1986). A comparative study of extraction methods for solar cell model parameters. *Solid State Electron* 29, 329–337. doi:10.1016/0038-1101(86)90212-1
- Chin, V. J., Salam, Z., and Ishaque, K. (2015). Cell modelling and model parameters estimation techniques for photovoltaic simulator application: a review. *Appl. Energy* 154, 500–519. doi:10.1016/j.apenergy.2015.05.035
- Cubas, J., Pindado, S., and Victoria, M. (2014). On the analytical approach for modeling photovoltaic systems behavior. *J. Power Sources*. 247, 467–474. doi:10.1016/j.jpowsour.2013.09.008

In conclusion, the Phang et al. method is identified as the most effective for both technologies, providing high-quality results with a strong agreement between experimental and predicted values.

Data availability statement

The original contributions presented in the study are included in the article/supplementary material, further inquiries can be directed to the corresponding author.

Author contributions

BB: Conceptualization, Data curation, Formal Analysis, Funding acquisition, Investigation, Methodology, Project administration, Resources, Software, Supervision, Validation, Visualization, Writing—original draft, Writing—review and editing.

Funding

The author(s) declare that no financial support was received for the research, authorship, and/or publication of this article.

Conflict of interest

The author declares that the research was conducted in the absence of any commercial or financial relationships that could be construed as a potential conflict of interest.

Publisher's note

All claims expressed in this article are solely those of the authors and do not necessarily represent those of their affiliated organizations, or those of the publisher, the editors and the reviewers. Any product that may be evaluated in this article, or claim that may be made by its manufacturer, is not guaranteed or endorsed by the publisher.

- De Blas, M. A., Torres, J. L., Prieto, E., and García, A. (2002). Selecting a suitable model for characterizing photovoltaic devices. *Renew. Energy*. 25, 371–380. doi:10.1016/S0960-1481(01)00056-8
- El Achouby, H., Zaimi, M., Ibral, A., and Assaid, E. M. (2018). New analytical approach for modelling effects of temperature and irradiance on physical parameters of photovoltaic solar module. *Energy Convers. Manag.* 177, 258–271. doi:10.1016/j.enconman.2018.09.054
- Femia, N., Petrone, G., Spagnuolo, G., and Vitelli, M. (2012). *Power electronics and control techniques for maximum energy harvesting in photovoltaic systems (Femia, N. et al; 2013)*. CRC Press, Taylor and Francis Group.
- Hussein, A. (2017). A simple approach to extract the unknown parameters of PV modules. *Turk. J. Electr. Eng. Comput. Sci.* 25, 4431–4444. doi:10.3906/elk-1703-14
- Karmalkar, S., and Haneefa, S. (2008). A physically based explicit I_{sc} – V_{oc} model of a solar cell for simple design calculations. *IEEE Electron Device Lett.* 29, 449–451. doi:10.1109/LED.2008.920466
- Khan, F., Baek, S. H., Park, Y., and Kim, J. H. (2013). Extraction of diode parameters of silicon solar cells under high illumination conditions. *Energy Convers. Manag.* 76, 421–429. doi:10.1016/j.enconman.2013.07.054
- Louzazni, M., and Belmahdi, B. (2022). “Analytical modelling approach of photovoltaic curves: analysis and comparison,” in *Lecture notes in networks and systems* (Springer Science and Business Media Deutschland GmbH), 562–572.
- Phang, J. C. H., Chan, D. S. H., and Phillips, J. R. (1984). Accurate analytical method for the extraction of solar cell model parameters. *Electron. Lett.* 20, 406–408. doi:10.1049/el:19840281
- Powell, M. (1968). *A Fortran subroutine for solving systems of non-linear algebraic equations*. undefined.
- Saleem, H., and Karmalkar, S. (2009). An analytical method to extract the physical parameters of a solar cell from four points on the illuminated I_{sc} – V_{oc} curve. *IEEE Electron Device Lett.* 30, 349–352. doi:10.1109/LED.2009.2013882
- Sera, D., Teodorescu, R., and Rodriguez, P. (2008). “Photovoltaic module diagnostics by series resistance monitoring and temperature and rated power estimation,” in *IECON proceedings (industrial electronics conference)* (IEEE Computer Society), 2195–2199.
- Sheraz Khalid, M., and Abido, M. A. (2014). A novel and accurate photovoltaic simulator based on seven-parameter model. *Electr. Power Syst. Res.* 116, 243–251. doi:10.1016/j.epr.2014.06.010
- Stornelli, V., Muttillio, M., de Rubeis, and Nardi, I. (2019). A new simplified five-parameter estimation method for single-diode model of photovoltaic panels. *Energies* 12, 4271. doi:10.3390/en12224271
- Villalva, M. G., Gazoli, J. R., and Filho, E. R. (2009). Comprehensive approach to modeling and simulation of photovoltaic arrays. *IEEE Trans. Power Electron.* 24, 1198–1208. doi:10.1109/TPEL.2009.2013862
- Wang, G., Zhao, K., Shi, J., Chen, W., Zhang, H., Yang, X., et al. (2017). An iterative approach for modeling photovoltaic modules without implicit equations. *Appl. Energy*. 202, 189–198. doi:10.1016/j.apenergy.2017.05.149
- Yahya-Khotbehsara, A., and Shahhoseini, A. (2018). A fast modeling of the double-diode model for PV modules using combined analytical and numerical approach. *Sol. Energy*. 162, 403–409. doi:10.1016/j.solener.2018.01.047
- Zaimi, M., El Achouby, H., Ibral, A., and Assaid, E. M. (2019). Determining combined effects of solar radiation and panel junction temperature on all model-parameters to forecast peak power and photovoltaic yield of solar panel under non-standard conditions. *Sol. Energy*. 191, 341–359. doi:10.1016/j.solener.2019.09.007

Nomenclature

Abbreviations

SDM	Single diode model
STC	Standard tests conditions
RMSE	Root mean square error
MBE	Mean bias error
NRMSE	Mean absolute percentage error
MAPE	Normalized root mean square error
AE	Absolute error
DDM	Double diode model
TDM	Third diode model
p-Si	Polycrystalline
m-Si	Monocrystalline
MPP	Maximum power point
GNI	Global normal irradiation (W/m^2)

Symbols

I-V	Photocurrent-voltage
U-V	Power-voltage
R_{sh}	Shunt resistance (Ω)
R_s	Series resistance (Ω)
I_{ph}	Photo-generated current (A)
I₀	Diode saturation current
α	Diode ideality factor
V_T	Thermal voltage
k	Boltzmann constant ($1.3806503 \times 10^{-23}$ J/K)
q	Electron charge ($1.60217646 \times 10^{-19}$ C)
I_{sc}	Short circuit current at STC (A)
V_{oc}	Open circuit voltage at STC (V)
I_{MPP}	Maximum power current of PV module (A)
V_{MPP}	Maximum power voltage (V)
V_T	Thermal voltage